This article has been accepted for inclusion in a future issue of this journal. Content is final as presented, with the exception of pagination.

Gear-Train-Enabled Ingestible Capsule System Toward Wireless Targeted Intestinal Biopsy

Michael A. Straker, Joshua A. Levy, Anika Prasanna, Patrick A. Sweeney, Justin M. Stine, *Member, IEEE*, Luke A. Beardslee, *Senior Member, IEEE*, and Reza Ghodssi, *Fellow, IEEE*

***Abstract*—Diagnosing gastrointestinal (GI) diseases affecting the small intestine is a prevalent healthcare challenge as traditional procedures require sedation and have limited small intestinal access. Ingestible capsule technologies have emerged as a promising minimally-invasive alternative to endoscopic procedures, offering access to the entire GI tract. However, biopsy capsules have yet to translate clinically due to their external stimulation or power requirements. Here, an ingestible low-power thermomechanical gear-train actuation system featuring a hybrid 3D-printed tissue scraper is demonstrated. The system easily interfaces with ingestible capsule-based electronics for on-command activation with a power requirement of 150-180 mW, a ∼40-80% power reduction compared to previously demonstrated prototypes. The tissue scraper features a 1 μm blade requiring 0.208 ± 0.053 N to penetrate phantom tumor tissue to a 500 μm depth. An average output force of 2.5 ± 0.8 N was demonstrated by the system, surpassing the necessary penetration force. Testing on ex vivo tissue showed a collection volume of 1.5 ± 1.2 mm^3 which is relevant for histological and genetic analysis. The device was integrated with ingestible electronics which wirelessly initiate activation; a necessary capability for future feedback-driven sampling. Overall, the biopsy system represents an advance toward autonomous small intestinal tissue biopsy, introducing a new paradigm for GI disease diagnosis. [2026-0013]**

***Index Terms*—Ingestible capsule, biopsy, 3D-printing, remote activation.**

Received 2 February 2026; revised 30 April 2026; accepted 20 May 2026. This work was supported by the National Science Foundation ECCS Program under Award 1926793. Subject Editor E. Meng. *(Corresponding author: Reza Ghodssi.)*

Michael A. Straker is with the Fischell Department of Bioengineering, the Institute for Systems Research, and the Fischell Institute for Biomedical Devices, University of Maryland, College Park, MD 20742 USA.

Joshua A. Levy is with the Institute for Systems Research, the Fischell Institute for Biomedical Devices, and the Department of Material Science and Engineering, University of Maryland, College Park, MD 20742 USA.

Anika Prasanna is with the Fischell Department of Bioengineering, University of Maryland, College Park, MD 20742 USA.

Patrick A. Sweeney is with the Department of Electrical and Computer Engineering, University of Maryland, College Park, MD 20742 USA.

Justin M. Stine is with the Institute for Systems Research, MATRIX Lab, A. James Clark School of Engineering, University of Maryland, California, MD 20619 USA.

Luke A. Beardslee is with the Institute for Systems Research, University of Maryland, College Park, MD 20742 USA.

Reza Ghodssi is with the Fischell Department of Bioengineering, the Institute for Systems Research, the Fischell Institute for Biomedical Devices, the Department of Material Science and Engineering, and the Department of Electrical and Computer Engineering, University of Maryland, College Park, MD 20742, USA, and also with the MATRIX Laboratory, A. James Clark School of Engineering, University of Maryland, California, MD 20619 USA (e-mail: ghodssi@umd.edu).

This article has supplementary downloadable material available at https://doi.org/10.1109/JMEMS.2026.37010227, provided by the authors.

Digital Object Identifier 10.1109/JMEMS.2026.3701022

I. Introduction

DIGESTIVE diseases are prevalent healthcare conditions globally, affecting in millions of individuals worldwide [1], [2]. Early detection of gastrointestinal (GI) diseases and their preceding conditions is vital for proper treatment, management, and prevention [3], [4]. A complicating factor in the diagnostic process is the overlapping symptoms or clinical presentation of GI diseases. For instance, ulcerative colitis and Crohn's disease both result in areas of inflamed GI tissue accompanied by symptoms such as vague abdominal pain [5], [6]. Often, to reach a definitive diagnosis tissue samples must be collected, or biopsied, for evaluation by a pathologist. A biopsy can reveal microscopic structural abnormalities such as mucosal degradation, dysplasia, and immune cell infiltration [3], [7], [8]. In a clinical setting, tissue samples are collected during endoscopy, an invasive procedure in which a doctor-operated fiber-optic camera navigates the GI tract to identify areas of concern and collect tissue with forceps inserted through the endoscope. However, these procedures have key drawbacks including high cost and sedation requirements.

Ingestible capsules are an emerging attractive alternative to endoscopy. In fact, studies have shown that patients prefer capsules to endoscopy for routine GI health screening [9], [10], [11], [12]. The first ingestible biopsy capsule was demonstrated in 1957, taking the form of a capsule embodiment tethered via a tube that could be used to aspirate tissue in regions of interest [13]. Location tracking was achieved through a combination of fluoroscopy and measuring the travel distance of the tube. The capsule contained a 17-gauge needle at the end of the tubing to perform tissue removal. More recently, wireless capsules have addressed the limitations of this design, removing the need for tethering and real-time external imaging [14], [15], [16], [17], [18]. The Pillcam is an ingestible video endoscopy capsule that has become a standard tool in gastroenterology [15], [16]. It provides end-to-end imaging of the entire GI tract, reaching remote regions like the distal small intestine, that traditional endoscopes cannot. Capsules equipped with optical, chemical, and physiological sensors are commercially available; however, devices with tissue sampling capabilities have yet to breach the prototype stage [14], [18]. Many ingestible biopsy capsules can be found in the literature, but their clinical translation is limited because they require real-time external monitoring and stimulation or exceed ingestible device power and size constraints. [19], [20], [21], [22], [23], [24], [25], [26], [27], [28], [29], [30], [31], [32], [33], [34], [35], [36], [37], [38], [39]. Devices must achieve an 11 mm x 26 mm form factor for clinical use, though prototypes with diameters of 13-14 mm and lengths exceeding 30 mm have reached preclinical large animal testing [40], [41],

1057-7157 © 2026 IEEE. All rights reserved, including rights for text and data mining, and training of artificial intelligence and similar technologies. Personal use is permitted, but republication/redistribution requires IEEE permission.
See https://www.ieee.org/publications/rights/index.html for more information.

Authorized licensed use limited to: University of Maryland College Park. Downloaded on July 02,2026 at 20:38:50 UTC from IEEE Xplore. Restrictions apply.

This article has been accepted for inclusion in a future issue of this journal. Content is final as presented, with the exception of pagination.

[42]. Further, commercially available ingestible sized batteries typically operate at currents of 60 mA or below. Exceeding these specifications can lead to battery degradation and limit its functionality for subsequent functions.

Magnetic actuation has been widely adapted for ingestible biopsy capsule designs because it requires no onboard energy source, has a rapid response time, can provide a means of orientation, and locomotion. Capsules capable of bulk tissue sampling [26], [32], [34] and fine needle aspiration [33] have been demonstrated. Researchers have also combined magnetic actuation with other mechanisms triggered by onboard electronics such as shape memory alloys (SMA) [37] and DC motors [43]. While these devices have demonstrated successful tissue resection, they require external magnetic fields to provide the driving force for tissue penetration and extraction. To generate these external fields, large electromagnetic coils [44], [45] or a permanent magnet actuated by a robotic arm [46], [47] are used. This greatly limits the potential for clinical translation, as it necessitates active external monitoring and trained operators, increasing costs. These shortcomings can be addressed by the development of an ingestible biopsy capsule that is triggered remotely by onboard electronics.

An ingestible biopsy capsule that can autonomously locate an area of interest and collect a sample without external activation requires a low power, battery triggered collection system. The prevailing approaches to developing biopsy modules compatible with untethered ingestible electronics involve electrically triggered release of stored mechanical energy or force transduction. Rehan et al. developed a device that utilized an SMA spring that would extend a rectangular fused filament fabrication printed sampling compartment to scrape the intestinal mucosa [25], [48]. The major limitation of this design was power efficiency, requiring 400 mW and connection to a non-ingestible external battery for remote operation. Park et al. developed a MEMS fabricated actuation module to complement a standard endoscopy capsule platform for tissue biopsy [49], [50]. The device featured a serrated silicon excising tool actuated by a crankshaft-style mechanism. Actuation was triggered by melting a polymer spring holding a torsion spring in place with an SMA rod. The authors demonstrated the feasibility of ingestible capsule integration by mounting the module in an endoscopic capsule prototype but never demonstrated remote battery activation. Moreover, the 160 mA (240 mW of power) used to actuate the SMA is far over the normal operating current of 60 mA from relatively large ingestible-size batteries. Our group previously demonstrated a biopsy module featuring a cam and follower actuator triggered by melting of an adhesive by an integrated microheater. The device could be triggered with a relatively low power 150 mW [51], however, this approach limits the volume of sample collected on the thin intestinal wall tissue and prolonged response time.

In this work, we present the sample collection unit for untethered pills (SCUUP), a novel low power, rotational biopsy module for sampling intestinal mucosa, enabling operation from a self-contained, battery powered ingestible capsule device (Figure 1). Previously, Song et al. [20] presented a biopsy device design featuring a gear train mechanism that was triggered by a tethered Bowden cable. The Bowden cable activates collection when the handle is mechanically

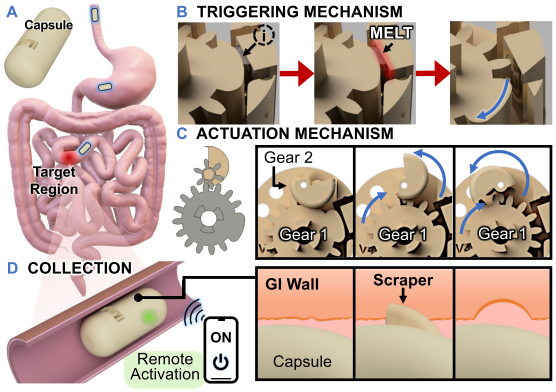

Fig. 1. (A) The biopsy module integrated with an ingestible device, travels to the target region in the small intestine (SI), where the onboard electronics trigger gear mechanism. (B) The adhesive (i) holding Gear 1 in place is melted allowing it to be rotated by a loaded torsion spring attached on its backside. (C) Gear 1 turns Gear 2 and the attached scraper 180°. The collecting tool. (D) The device is remotely activated, and the scraper is actuated into the GI wall, collecting a sample of the mucosa.

compressed by the operator. The SCUUP advances the use of the gear train design, addressing key systems engineering challenges by reducing the power and instantaneous current draw needed to activate the device, allowing it to operate wirelessly along with onboard electronics for targeting, using a single battery. The device is swallowed and travels to the target region in the small intestine (Figure 1A). Then, the SCUUP is triggered by the melting of an adhesive (Figure 1B), allowing a pre-loaded torsion spring to actuate the gear train (Figure 1C). GI tissue is then collected by a scraper attached to Gear 2, bringing it back into the capsule shell for storage until it exits the GI tract and can be retrieved (Figure 1D). The device is fabricated by combining liquid crystal display vat photopolymerization (LCD-VVP) and direct laser writing (DLW) 3D-printing technologies to create a gear-train actuated system featuring meso- to micro-scale features. This fabrication approach allows for the creation of a sharp, mechanically robust microscale blade for enhanced tissue penetration. To our knowledge, this is the first functional use of DLW printed microblades for untethered biological tissue sampling. Mechanical and electrical characterization of the system and its components were conducted to evaluate the force output and power requirements. The SCUUP was evaluated on agarose tissue phantoms and *ex vivo* porcine tissue, demonstrating the ability to collect samples that are compatible with clinical techniques for assessing disease state. Finally, the system was integrated with ingestible electronics and validated on phantom tissue as a proof-of-concept. Overall, the biopsy module presented here has the potential to enable intestinal tissue biopsy from operator independent ingestible capsule platforms, establishing a new paradigm of GI health diagnostics.

II. Materials and Methods

A. Module Fabrication, Assembly, and Capsule Integration

The biopsy module consists of a base, a corrosion-resistant 302 stainless-steel torsion spring (McMaster-Carr, Elmhurst, IL, USA), a ~70-90 Ω resistive heater, a drive gear (gear 1), and a pinion (Gear 2) which is connected to the tissue scraper. The microfabricated thin film gold heater described in

Authorized licensed use limited to: University of Maryland College Park. Downloaded on July 02,2026 at 20:38:50 UTC from IEEE Xplore. Restrictions apply.

This article has been accepted for inclusion in a future issue of this journal. Content is final as presented, with the exception of pagination.

Levy et al. [52] was mounted to transparency film and fixed to a slot in the base with ethyl cyanoacrylate adhesive (Newell Brands, Atlanta, GA, USA). Wires or pin receptacles were fed through channels on opposite sides of the heater slot and connected electrically via silver conductive epoxy adhesive (MG Chemicals, Burlington, Ontario, Canada). The torsion spring was loaded by immobilizing one end in a slot in base and the other end in the slot of Gear 1. Gear 1 is then rotated 90-180° counterclockwise from its starting position and fixed to the heater with ethylene-vinyl acetate (EVA) adhesive (The Gorilla Glue Company, Cincinnati, OH, USA). The module is finally enclosed in a 3D-printed shell. To test the modules, wires connected the heater, or receptacles were connected to a DC power supply (Agilent, Santa Clara, CA, USA), limiting peak voltage and current to 3.3 V and 60 mA, respectively, was used to initially demonstrate module actuation.

The mechanical gears, base and shell were printed using surgical guide resin (Formlabs Inc., Somerville, MA, USA), a biocompatible resin, and the Phrozen Sonic Mini 8K Resin (Phrozen Tech Co., Ltd., Hsinchu City, Taiwan) LCD VPP. The gear design features a 9 mm drive gear (Gear 1) with 16 teeth and a pinion (Gear 2) of 4 mm with 6 teeth. Thus, the gear ratio of the system is 0.375.

The modules were integrated with the custom PCB and 2L76 battery (Energizer, St. Louis, MO, USA) via 30-AWG wires. The components were packaged in an LCD VPP printed resin shell. An iOS device connected to the PCB via the SiConnect application allowing for wireless transfer of commands through Bluetooth.

B. Heater Fabrication and Integration

Microheaters were fabricated using photolithography and ebeam metal deposition. A 1 mil flexible polyimide film (Kapton®, DuPont, Wilmington, DE, USA) was first adhered to a silicon carrier wafer. A layer of positive photoresist was spin coated on to the wafer and exposed UV exposed for patterning. A 20 nm layer of chromium was deposited using the Angstrom Ebeam Evaporator (Angstrom Engineering, Kitchener, Canada) to act as a seed layer to promote substrate adhesion. This was followed by another deposition step to deposit another 100 nm of gold. Films were subsequently sonicated in acetone for approximately 1 hr to lift off photoresist and produce the heater traces. Heaters were cut from the bulk film and adhered to transparency film. Films were then folded to create a 90° angle between the pads and concentric spiral traces of the heater.

C. Tissue Scraper Fabrication

The tissue scrapers were created using hybrid 3D-printing techniques combining printing techniques, first by printing custom base pieces using LCD-VPP 3D-printing. The base structures feature a semi-cylindrical hollow vestibule for storing collected samples and a rectangular fitting for integration with Gear 2. Sharp tapered blades were then printed on top of the structure by DLW 3D-printing using the NanoOne 1000 2PP 3D-Printer (UpNano, Vienna, Austria) with a 10x objective lens and UpPhoto resin (UpNano, Vienna, Austria). UpPhoto resin is ISO 10993-5:2009 biocompatible. The blades of the scrapers were printed with a 15° bevel angle from a 200 μm base up to a maximum height of ~ 650 μm. Scraper blades were printed 100 μm into the 3D-printed base structure ensure proper integration. To achieve alignment between the blade and base, a reference point at the center of the bottom edge of the blade's inner face was manually aligned with a fixed reference point on the inside edge of the base receptacle using the printer's viewing interface prior to printing. The total print time of a blade was ~25 min. Scrapers were subsequently cleaned in an isopropanol (IPA) bath for 30-60 min.

D. System Force Testing

The mechanical force output of the module was measured using a custom built loadcell setup. A 5kg load cell (NOYITO NOLDKHX711-5, Changzhou Xuchuang Information Technology Co., Ltd., China) was connected to an HX711 analog-to-digital converter (ADC) and an Arduino Uno board. Custom fixtures were printed using a Prusa i3 MK3S + (Prusa Research, Czechia) and polylactic acid (PLA) filament. Modules were fixed in custom 3D-printed holders and immobilized in EVA, then deployed into the stationary load cell.

E. Scraper Penetration and Retraction Force Characterization

Agarose tissue phantoms of 0.2 %, 1.28%, and 3.07% w/v were fabricated by dissolving 0.08, 0.512, and 1.23 g of agarose powder (Fisher Scientific, Hampton, NH, USA) in 40 mL of deionized water. Penetration and retraction forces were measured using an Instron 5942 universal testing machine (UTM; Norwood, MA, USA) with a crosshead speed of 1 mm/min to minimize inertial effects. Samples were translated into the tissue 500 μm to ensure proper penetration and then retracted until full separation was observed.

F. Device Agar and Tissue Collection

Agarose tissue phantoms of 1.28% were fabricated by dissolving 0.512g of agarose powder (Fisher Scientific, Hampton, NH, USA) in 40 mL of deionized water and refrigerated until solidified. Sections of ~ 20 × 30 mm were cut from the bulk for module testing. Porcine small intestinal tissue was procured from Animal Biotech Industries (Doylestown, PA, USA). Samples were freshly excised and subsequently frozen from postmortem animals. Tissue samples were cut into approximately 20 × 30 mm sections and fixed to agarose phantom backings. Modules were then deployed onto tissue sections for sample collection.

G. Statistical Analysis

The experiments were performed in independent replicates, with the number of repetitions indicated in the corresponding figure captions. Data are reported as mean ± standard deviation to reflect the variability observed across replicates. Standard deviation was calculated to assess the reproducibility and consistency of the measurements.

Authorized licensed use limited to: University of Maryland College Park. Downloaded on July 02,2026 at 20:38:50 UTC from IEEE Xplore. Restrictions apply.

This article has been accepted for inclusion in a future issue of this journal. Content is final as presented, with the exception of pagination.

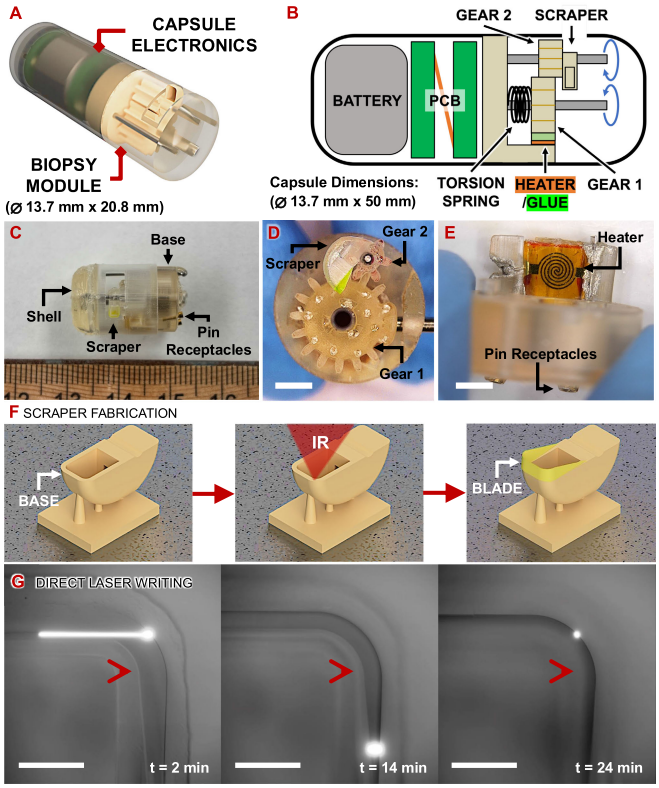

Fig. 2. (A) CAD rendering depicting a SCUUP module integrated with wireless capsule electronics. (B) A 2-dimensional schematic of the SCUUP integrated capsule. (C) Photograph of the SCUUP module (final dimensions: ø 13.7 mm x 20.8 mm). (D) Pictures of the internal gear mechanism and (E) integrated Au heater for triggering. (scalebars: 3 mm) (F) Renderings depicting the fabrication process of the scraping tool. (G) Images depicting the 2-Photon Polymerization 3D-printing process of the scrapers. The red arrow indicates the position of the blade during printing (scalebars: 500 μm).

III. Results and Discussion

A. Actuator Design and Fabrication

The SCUUP (Figure 2A) features a modular design housing all actuator and tissue sampling components in a single 3D-printed shell compartment, with electrical connections facilitated by embedded pin receptacles on its base. This allows it to be evaluated and refined independently, while remaining readily configurable for capsule electronics of varying designs. An overview schematic of a fully assembled capsule is shown in Figure 2B. The capsule contains: an ingestible battery for powering the electronics, a PCB for receiving wireless signals and triggering actuation, and the SCUUP actuator components. Using flexible polyimide-based heater fabrication, 3D-printed channels for housing electrical interconnections, and a gear assembly that fits within the actuator module footprint enable significant miniaturization.

Once assembled, the entire capsule measures 50 mm in length and 13.7 mm in diameter, with the biopsy module (Figure 2C) occupying only 42% of the total volume and the remainder occupied by the electronics and battery. The module base serves multiple functions: (i) providing channels for electrical interconnects between the heater and pin receptacles, and (ii) acting as a mechanical anchor for the module, ensuring stability during operation. The gear-train system, illustrated in Figure 2D, was selected for its flat, compact profile and ability to efficiently transfer torque from the spring to the tissue scraper throughout actuation. The rotational motion allows the scraper to translate out of the capsule enclosure, collect a sample, and return for storage. The ~ 70 Ω Au-resistive heater (Figure 2E), described previously in Levy et al. [52], is flexible, allowing it to be nested in a compact slot in the base. It is electrically connected to the pin receptacles through silver epoxy-filled conductive channels.

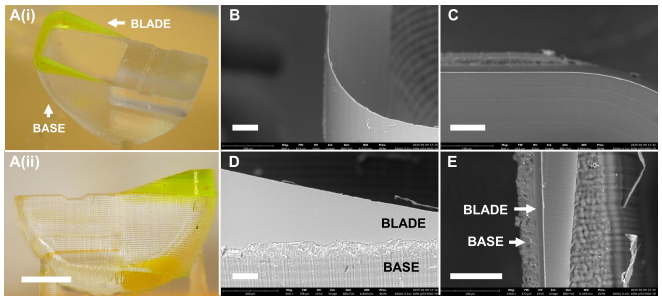

Fig. 3. (A) Perspective view (i) and sideview (ii) optical images of the scraper after printing (scalebars: 1 mm). SEM Images of the fabricated scraper blade for tissue penetration and collection. (B) Perspective view of blade tip. (C) Top view of the blade tip revealing tip thickness of ~ 1 μm. A sideview (D) and top view (E) of the interface between 3-D printed portions of the scraper. (SEM scale bars: 100 μm).

The gears, base, and shell were fabricated using biocompatible surgical guide resin through LCD vat photopolymerization (LCD-VPP). Due to the 22 μm X and Y resolution of standard LCD-VPP, achieving sharp, single-micron features is difficult. Therefore, to fabricate the tissue scraper, the scraper base was printed with LCD-VPP (Figure 2F and Figure S2), then the scraper blade was printed directly onto the base with UpPhoto resin utilizing DLW. Both the UpPhoto resin used for the blade and Surgical Guide resin in the base are ISO 10993 compliant materials and non-cytotoxic. Figure 2G shows the printing process of the blade, where the laser scans over the resin, creating each layer of the structure. Each successive printed layer is made narrower, forming the pyramidal shape of the blade that tapers to a sharp point. During the print, the laser power was set to 50 mW for infills at a scan rate of 600 mm/s throughout the print, with the voxel height of 8.87 μm and voxel width of 0.735 μm. When printing shape outlines or finer features, the laser power and scan rate are modulated to 32 mW and 100 mm/s respectively. At 2- and 14-min print time, the laser can be observed creating the base and mid-section of the blade with infills at widths of 130-200 μm. At 24 min, nearing the zenith of structure, features are likely produced by multiple outlines as the feature width is reduced to < 10 μm.

B. Tissue Scraper Characterization

A major challenge for electromechanical biopsy capsules is generating enough pressure at the interface of the GI tissue to effectively and safely sever tissue samples. This is largely due to manufacturing limits in creating sharp and mechanically robust structures for cutting. Literature has shown that to cut small intestinal tissue, a destructive stress of ~1.2 MPa [53] must be applied throughout contact where tip thickness

Authorized licensed use limited to: University of Maryland College Park. Downloaded on July 02,2026 at 20:38:50 UTC from IEEE Xplore. Restrictions apply.

This article has been accepted for inclusion in a future issue of this journal. Content is final as presented, with the exception of pagination.

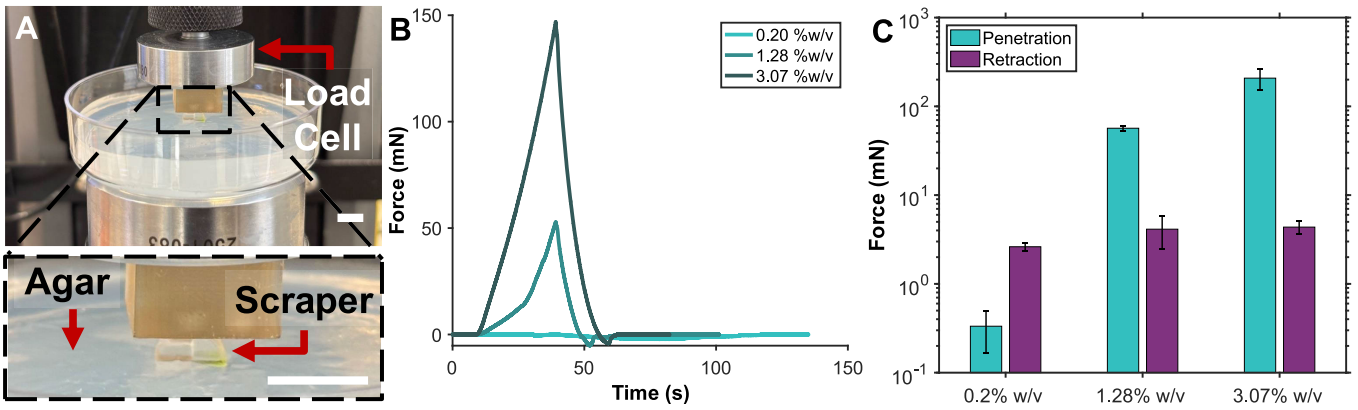

Fig. 4. (A) An image depicting the experimental setup in which the scoop is driven into and subsequently pulled out of an agarose phantom. (scale bar: 6mm) (B) Example results showing the penetration and retraction force measured by the force tester on the agar phantoms of varying stiffness. (C) A bar graph summarizing the results of the characterization (n= 3). The y-axis represents the log of the Force in mN.

is inversely proportional to the minimum force required for penetration, and higher tip sharpness reduces the force necessary to induce destructive stress and penetration. Typically, collection structures are fabricated from metals utilizing subtractive machining techniques achieving thicknesses of 30-100 μm [20], [21], [32]. Moreover, the 19-25 G hollow needles traditionally used for fine needle aspiration biopsy have wall thicknesses of ~100-200 μm [54], [55]. The tip sharpness of the capsular biopsy collection tools report in literature were 30 μm [37], while typically surgical cutting tools feature a tip sharpness of 5-15 μm [56], [57], [58], [59], [60]. In this work, the scraper blade is fabricated from a photopolymer resin with a flexural strength of 127 MPa and maximum compressive strength of 132-142 MPa [61]. The pyramidal cross-sectional design (seen in Figure 3A) of the scrapers also serves to support structural stability and reduce bending due to moments applied at the blade tip during actuation. A bevel angle of 15° was chosen for the blade to mimic of the geometry of 19-22 G biopsy needles, reducing drag throughout penetration.

To assess the sharpness of the fabricated scraper blade, scanning electron microscopy (SEM) was conducted on scraper samples before final assembly. Evaluation of the micrographs revealed that the blades had a sharpness of approximately 1 μm (Figure 3B-C). Given this thickness and the maximum expected vertical distance, the scraper will travel outside of the capsule to be < 1 mm, the initial area of contact of the tissue scraper can be estimated to be 0.25 mm^2. The scraper blade is printed 100 μm into the LCD-VPP 3D-printed base, ensuring a stable bond and fusion of the two materials, as is shown in the micrographs of the blade-base interface (Figure 3D-E).

To validate the mechanical robustness of the scraper blade and its ability to penetrate tissue of different stiffness, it was tested on agarose phantoms of varying stiffness. Agarose phantoms have been widely used to mimic mechanical properties of biological tissue and as templates for in vitro testing of microscale structures for tissue penetration [62], [63], [64]. Studies have found that diseased tissue including chronically inflamed and carcinogenic tissue can have higher modulus than healthy tissue due to inflammation-induced fibrosis and tissue restructuring due to mutations [65], [66], [67], [68]. Phantoms were fabricated with concentrations of 0.2, 1.28, and 3.07 % w/v [69] to simulate intestinal mucosa (E = 2.6 kPa) [66], inflamed tissue (E = 16 kPa) [66], and tumor tissue stiffness (E = 40 kPa) [65], respectively. Samples were translated by a mechanical tester at a crosshead speed of 1 mm/min into the phantom until the blade reached full penetration (~ 500 μm) and retracted until full separation was achieved (Figure 4A). Penetration forces scaled with the increase in phantom concentration (Figure 4B). The maximum penetration forces of the scraper (Figure 4C) were 0.333±0.16, 56.7±3.7, 208±53 mN for 0.2, 1.28, and 3.07 % w/v phantoms respectively; while the retraction forces were 2.62±0.26, 4.13±1.6, 4.36±0.73 mN. While there was a significant increase in the penetration force between the inflamed and tumor tissue phantom penetration, the relative increase in retraction force observed was less than 2×. Although the scraper performed reliably in the phantoms, further characterization of the scraper stability is an important future step. Specifically, characterization of resistance to perpendicular force loads at the blade-base interface could aid in validating and optimizing the fabrication process. Moreover, a quantitative assessment of run-to-run variation in the blade–base alignment procedure was not performed in this study and should be investigated in future work to evaluate process tolerances, reproducibility, and manufacturability.

C. Gear Train Actuator Characterization

The actuation of the biopsy module is triggered by the melting of EVA that immobilizes the drive gear. A preloaded corrosion-resistant steel torsion spring stores and releases the mechanical energy needed to actuate the biopsy mechanism. The success criteria for the actuator are (1) the pinion connected to the tissue scraper must complete the 240° of rotation necessary to rotate above and then back into the capsule shell, and (2) maintain the necessary destructive stress over the duration of its actuation outside of the capsule. Based on the gear train and module design, the expected output force can be calculated using Equation 1, which is derived from fundamental mechanics [70], [71], noting that the torque of each individual gear is equal (Figure S3). In this equation, F

Authorized licensed use limited to: University of Maryland College Park. Downloaded on July 02,2026 at 20:38:50 UTC from IEEE Xplore. Restrictions apply.

This article has been accepted for inclusion in a future issue of this journal. Content is final as presented, with the exception of pagination.

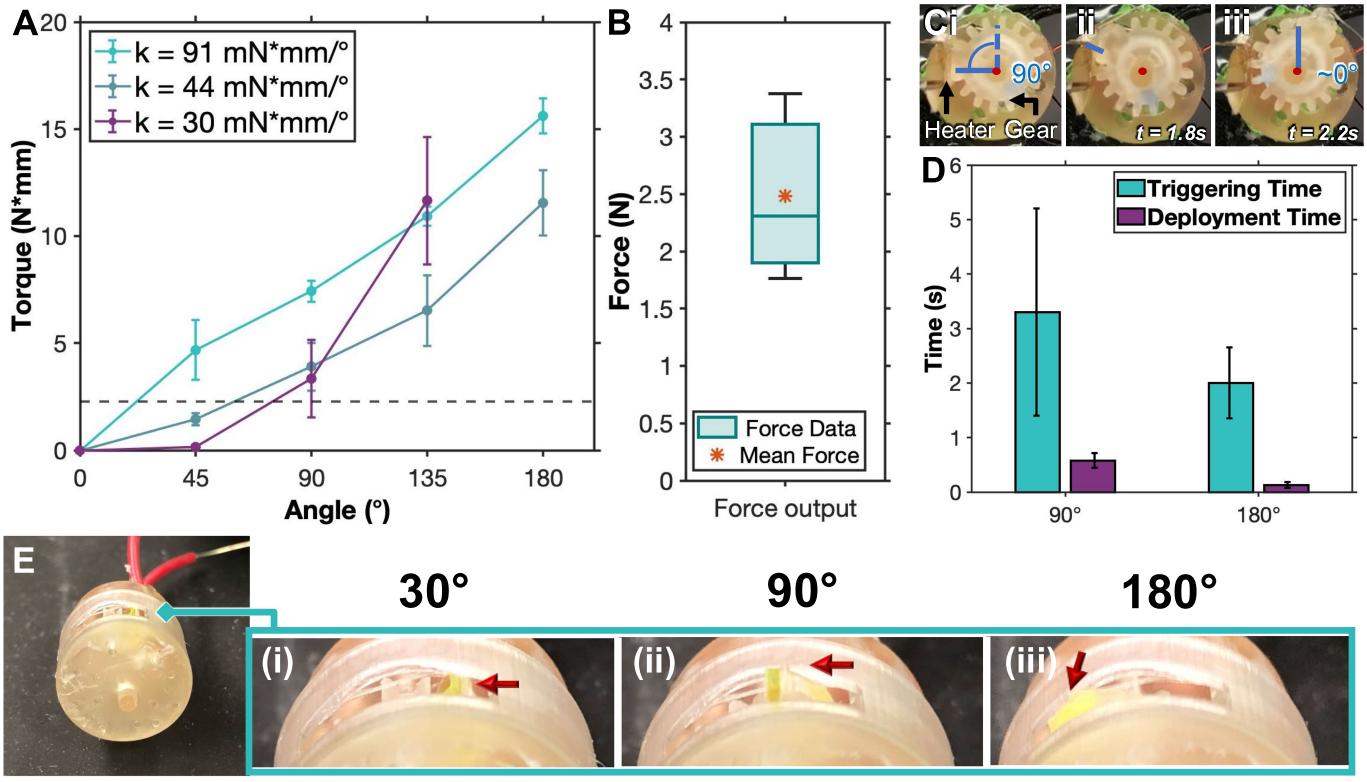

Fig. 5. (A) Results of torque characterization of potential stainless-steel springs with varying stiffness (k). The dotted line represents the minimum torque to cut tissue. (n= 10) (B) Box and whisker plot showing peak output force of deployed collector. (n= 3) Images depicting the triggering of the internal drive gear actuation of the drive gear before (C.i), at the beginning (C.ii) and end (C.iii) of deployment. The solid blue line indicates the edge of the connection portion of the gear as it rotates. (D) Results of the triggering characterization of modules triggered at 90 and 180° loading angles. (E) Images demonstrating the module firing, resulting in the scraper rotating out and back into the capsule enclosure.

represents the force, r represents the radius, and τ represents the torque of the respective subcomponents of the system.

$$F_{Output} = \tau_{Spring} * \frac{r_{Gear2}}{r_{Gear1} * r_{Scraper}} \quad (1)$$

From Equation 1, the output force applied by the scraper on the tissue will be 0.1× the force provided by the drive gear (Gear 1). The drive gear force will be equal to the torsion spring force output at any given deflection angle. Three potential stainless-steel torsion springs were evaluated to identify which would provide the torque and the deflection angle necessary for reliable operation of the module (Figure S3). Results of the experiment (Figure 5A) show that spring 1 (k = 91 mN-mm/°) can produce the necessary cutting torque when above the 45° loading angle, while spring 2 (k = 44 mN-mm/°) and spring 3 (k = 30 mN-mm/°) must be loaded to ~90°. Further, spring 3 demonstrated unstable force output at 0-90° and deforms at deflection angles > 135°. Spring 1 was selected for its stability and to maximize torque throughout actuation. Using spring 1, the average force output of the system was 2.5±0.8 N (n= 3) (Figure 5B and Figure S4) when loaded to a deflection angle of ~180°. The force output when loaded at ~90° was 1.6±0.4 N (n= 3) (Figure S4). The results indicate that the module supplies sufficient force to induce local destructive stress and penetrate small intestinal tissue upon contact. Using Equation 2 where P_D is destructive pressure, F is force, and A is the estimated contact area of tissue scraper tip, we calculate the equivalent to be 300 mN of force. Thus, penetration is achievable given the force output results.

$$F = P_D * A \quad (2)$$

It is important that both triggering of the module and tissue scraping actuation occur rapidly to mitigate delay of device activation resulting in offsite tissue collection. Additionally, rapid cutting mitigates the effects of tissue deflection due to induced force. The triggering and actuation time of the internal drive gear mechanism was evaluated to ensure rapid operation (Figure 5C). The heater was previously demonstrated for triggering a drug delivery actuator producing force loads < 1 N [52], [72]. Heat dissipation from the heater into the EVA causes the material to soften at optimal temperature of 88 °C. However, hot melt adhesive modulus and resistance to peeling from a substrate decreases > 7× as it approaches optimal softening temperature, leading to quicker release times [73]. The average triggering time of the module (Figure 5D) at 90° and 180° loading angles were 3.3±1.9 s and 2.0±0.65 s, while the deployment times were 0.58±0.19 s and 0.13±0.06 s, respectively (n= 5). This result suggests that collection would occur at a rapid rate relative to the expected translation speed of an object in the small intestine due to peristalsis (1.4 cm/min [74], [75]). The average rotational velocity of the drive gear ranges from 50-115 RPM or 5.2-12 rad/s. Considering the gear ratio (0.375), this would correspond to a rotational velocity of ~130-300 RPM or 12-31 rad/s for the tissue scoop. The range of rotational speeds falls within operating parameters

Authorized licensed use limited to: University of Maryland College Park. Downloaded on July 02,2026 at 20:38:50 UTC from IEEE Xplore. Restrictions apply.

This article has been accepted for inclusion in a future issue of this journal. Content is final as presented, with the exception of pagination.

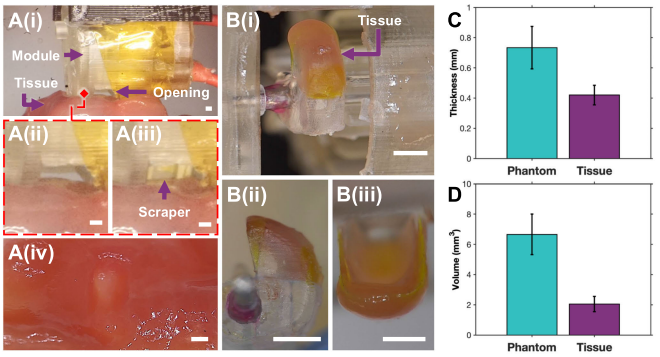

Fig. 6. (A) Photographs of (i) the module sampling test on ex vivo tissue setup. Images showing (ii) the shell opening before deployment and (iii) the scraper during deployment. (iv) Shows the tissue after testing depicting the sampling area. (B) Photographs of the back (i), sideview (ii) and top (iii) of tissue scraper after collection. (C) Results showing the average thickness of the samples collected from the tissue phantoms and ex vivo tissue. (D) Results showing the average volume of the tissue phantoms and ex vivo tissue. (scalebars: 1 mm).

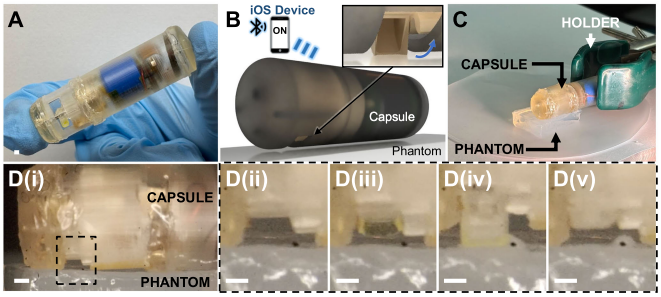

Fig. 7. (A) A photograph of the ingestible biopsy capsule. (B) A CAD rendering depicting the experimental setup where integrated biopsy capsule is triggered by a Bluetooth signal sent from an iOS device. (C) A photograph of the ingestible biopsy capsule. (D) Photographs of the capsule collection experiment (i) showing the capsule opening (ii) and the tissue scraper traveling out of the capsule (iii) into the phantom (iv) and bring tissue back into capsule enclosure (v). (scalebars: 1 mm).

(9.81-39.25 rad/s) of tethered rotational capsules demonstrated to collect intestinal tissue with cutting blades 100x thicker (0.1 mm) than the scoop [20]. Variation in deployment times was due to inconsistent application of EVA to immobilize the spring leg on the microheater. Higher volumes of EVA resulted in longer deployment times. Additionally, process variations of microheater resulted in resistance variation between 70-75 Ω. Thus, modules were triggered using current values between 50-60 mA and a power output of 150-180 mW, which is roughly 40-80% less than other wireless electromechanical biopsy capsules reported in literature [21]. This power output fits within the 180 mW limit of ingestible-sized batteries, making them compatible. Further, operating for 2-5 seconds consumes 5-12.5 mWh of the total 480 mWh energy capacity of the battery, allowing for ~97% of the battery energy to be applied to other capsule functions, such as sensing.

D. Device Sample Collection Characterization

To validate the ability of the device to sample small intestinal tissue, modules were deployed onto agarose tissue phantoms (Figure S5) and *ex vivo* small intestinal porcine tissue (Figure 6A). Samples collected from the agarose phantoms were on 733 ± 280 μm thick on average (n= 3) while samples collected from *ex vivo* porcine tissue were 323 ± 20 μm thick on average (n= 3). The differences in sample thickness are likely due to the overall thickness of the *ex vivo* intestinal tissue as well as its relative increase in elasticity. Typically, porcine GI tissue ranges from 1.15-2 mm in thickness before reaching the outermost layer (serosa), with the mucosa ranging from 0.45-1.5 mm in thickness [76], [77]. Human small intestinal wall thickness ranges from 2-3 mm [78], [79]. Moreover, the inner GI wall is lined with a tightly connected monolayer of epithelial cells which are approximately 7.2-7.9 μm in diameter, followed by the connective tissue of the lamina propia [80]. Full thickness samples taken from areas next to the biopsy site were 0.5-1.3 mm thick. We can expect that at this depth, mucosal epithelial tissue as well as cells from the lamina propia would be successfully collected [81]. As such, in histological staining of the samples collected from this depth could reveal pathological microstructural features such as mucosal disruption or shallow crypts, which are indicative of diseases IBD and celiac disease respectively [82], [83]. Agar samples collected by the module ranged from 4.0-9.4 mm^3 with an average of 6.7 ± 2.7 mm^3, while tissue samples collected ranged from 0.4-2.8 mm^3 with an average of 1.5 ± 1.2 mm^3. While less than volumes collected by traditional biopsy forceps, these results fall in the 1-5 mm^3 range of samples suitable for histological evaluation by a pathologist [84], [85], [86]. Moreover, studies report that 2000 cells, an estimated volume of 1.8×10^{-4} mm^3, is the minimum quantity necessary for reverse transcription polymerase chain reaction (RT-PCR), a laboratory technique commonly used in screening for disease-specific genes [87]. While these results demonstrate the success of the module to excavate and collect samples from a static tissue, conditions such as the presence of fluid, active peristaltic contractions, and capsule orientation may alter the modules performance. Evaluating the reliability of the system in a more complete and dynamic small intestinal environment, for which tissue contact conditions and anchoring will become important factors, is imperative to assess in future studies. Moreover, future studies will validate the device using freshly excised porcine intestinal tissue rather than the stiffer pre-frozen tissue. Freezing and thawing tissue has been shown to increased tissue stiffness and decreased elasticity [88]. Fresh tissue may therefore require lower penetration forces and greater displacement to achieve cutting and tearing. Investigating these differences will inform device optimization and mitigation of potential failure modes.

E. Capsule Integration and Benchtop Validation of Biopsy Capsule

To demonstrate the biopsy module in a wireless ingestible capsule device, the actuator was integrated with a button cell battery and previously developed ingestible PCB electronics featuring an electrochemical analog front end (AFE) and a Bluetooth microcontroller (Figure 7A and Figure S6) [89]. The AFE allows for the interpretation of the electrical input from sensors connected to it. Based on these measurements, a logic is set to toggle a switch connecting the heater to battery power

Authorized licensed use limited to: University of Maryland College Park. Downloaded on July 02,2026 at 20:38:50 UTC from IEEE Xplore. Restrictions apply.

This article has been accepted for inclusion in a future issue of this journal. Content is final as presented, with the exception of pagination.

once a condition or the threshold value is met. This proof-of-concept demonstration focuses on successful integration of the onboard triggering elements, and as such, the capsule features no sensing element. Instead, the capsule wirelessly connects to an iOS device (Figure 7B) via a Bluetooth antenna on the PCB enabling activation without a tethered connection or external magnetic field [90]. Previously, the Bluetooth antenna was characterized for its ability to transmit through a tissue analog demonstrating that it could transmit up to 70 cm through a tissue analog before signal attenuation caused failure to reach the -100 dbm threshold to communicate with a standard Bluetooth receiver [89]. Thus, we expect that the capsule can successfully communicate with a device outside of the patient. A voltage regulator integrated on the PCB maintains a voltage of 3.3 V to the heater for a preset 30 seconds. The capsule was tested on an agarose phantom (Figure 7C-D) where it collected a ~0.82 mm thick, ~3.2 mm^3 sample. This sample fits within the previously mentioned specification range of samples that can be used for diagnostic tests such as histology and RT-PCR [84], [87].

Overall, this successful demonstration represents a significant step toward a fully automated capsular biopsy system. The significant reduction in operating power (40-86%) requirement of the SCUUP compared to previously demonstrated thermo-mechanical biopsy modules (240-1430 mW [21], [25], [48], [49], [91]) has enabled the first demonstration of a Bluetooth-triggered biopsy capsule. To the knowledge of the authors, this is the first demonstration of an untethered ingestible tissue biopsy capsule powered from a single integrated ingestible battery. The 1.5-6.7 mm^3 average sample collection size provides sufficient biological material for key diagnostic benchtop procedures. Sensor integration and implementation of this device *in vivo* would allow for user independent site-specific tissue sampling in remote regions of the GI tract such as the small intestines. The electronics featured in this device have demonstrated successful feedback-driven operation based on sensor readings reaching a preset threshold [90].

Miniaturization is a critical factor in the development of ingestible capsules, and the risk of bowel retention limits the application of capsules with diameters < 11 mm and approximately 32 mm in length. The SCUUP was developed to interface directly with the capsule electronics and currently has a 13.7 mm outer diameter. The gear train actuation mechanism can readily be scaled to meet the required reduction in size by reducing the diameter of the gears and torsion spring. To achieve the overall length limit, the wireless biopsy capsule prototype would require a 14 mm overall reduction. The gears were lengthened to mitigate the risk of mechanical failure due to induced gear tooth misalignment from the reaction forces during actuation. Utilizing more mechanically robust materials with higher tensile strength such as polyetheretherketone (PEEK), silicon, and stainless steel would allow for shorter gears, greatly reducing capsule length. Additionally, the micro-heaters can be reduced in size as heaters of 1-3 mm diameter have been shown to effectively melt EVA [72]. Further, the prototype can be optimized by replacing both 2L76 battery and stainless steel springs with more compact alternatives. Successful miniaturization of the biopsy module to a 2-3 mm length scale would enable the inclusion of multiple modules in a single capsule, for repeated measurements. Maintaining proper orientation with the GI wall is another important factor in ensuring proper sampling. The current capsule design operates passively without direct mechanisms for positioning or avoiding debris, which is a limitation. Ingestible capsules are typically administered in a fasted state, removing food obstructions from the bowel. Under these operating conditions in the small intestine, we expect contractions due to peristalsis will maintain a contact pressure equivalent to 0.5-2.5 N/m and proximity to the bowel wall [92], [93]. However, this needs to be assessed experimentally, and the role of contact pressure on the sampling performance of the SCUUP will be investigated to ensure collection reliability and risk of perforation in future studies. This limitation can be address by integrating an anchoring system into the capsule to maintain stable contact with the GI wall. Selective bioadhesive patches, robotic hooks or stents can be deployed utilizing sensor feedback-based activation as well. Additionally, sample preservation is critical in the effective operation of sampling capsules, as proteins necessary for subsequent staining can quickly degrade. Transit through the intestines can range from 12-78 hours [53]. To mitigate these effects, further development of this design will include sealing and preservation components to ensure samples are not contaminated or degraded as the capsule exits the body. Sealing and selective opening of the sampling cavity can be achieved by attaching a polydimethylsiloxane (PDMS) hatch coverings to the drive gear allowing it to slide along the internal surface of the capsule enclosure while aligning its motion with the actuation of the scraper, closing the opening after collection. Passive strategies utilizing PDMS for in situ capsule sealing have shown success in preventing leaking and cross contamination in microbiome sampling applications [94], [95]. Further protection of the capsule cavity from contamination prior to entering the small intestine can be achieved through the use of enteric coatings which selectively target this region [96]. Non-toxic fixative options such as ethanol have been proposed as candidates for integration with ingestible sampling devices [91]. Moreover, to validate capsule sealing and investigate effects of long term residency, the device must be tested in gastrointestinal fluids or analogs to validate its long term viability. Following the benchtop evaluations, the potential for bowel obstruction, perforation, and collection mechanism failure must be evaluated *in vivo*. Another critical safety factor that must be evaluated is the capsule's temperature during operation. Tissue can suffer instant damage when elevated to temperatures above 60 °C [97] while assessment of GI tissue elevated to temperatures below this threshold required exposure for > 15 min to induce damage [98]. With the heaters reaching temperatures exceeding the 88 °C EVA melting temperature, it is important that future work directly measures capsules temperature during heating. Moreover, heat generated from PCB operation has potential to contribute to the elevation of the overall capsule temperature. An initial assessment of the temperature increase of the capsule (Figure S7) considers the power output of the heater, necessary run time, the estimated mass of the capsule, and specific heat capacity of related resin material that comprises most of the capsule. The result suggests that the overall capsule temperature would not increase more than

Authorized licensed use limited to: University of Maryland College Park. Downloaded on July 02,2026 at 20:38:50 UTC from IEEE Xplore. Restrictions apply.

This article has been accepted for inclusion in a future issue of this journal. Content is final as presented, with the exception of pagination.

2 °C during the 5 sec operation time, making it unlikely to cause tissue damage. However, the potential localized heating effects must be determined experimentally. To mitigate dangerous heat transfer, thermally insulative materials such as PEEK, silicone, and polyimide could be added to the capsule tissue interface. The hybrid 3D-printing fabrication techniques employed here enabled robust microscale structures to directly interface with mm-scale components for enhanced penetration and sample collection. While LCD-VPP and DLW can produce high resolution features, they are limited in scalability and material selection. To address this, techniques such as micromolding and microfabrication can be explored as alternatives for creating these multiscale components.

IV. Conclusion

In this paper, we present the first fully self-contained, wireless rotational biopsy module capable of on command tissue sampling from a battery-powered ingestible capsule device. The module is achieved by utilizing LCD-VPP 3D-printing and DLW 3D-printing to create a 1 μm sharp scraping tool that is mechanically robust enough to penetrate tissue. An internal gear train mechanism is used to actuate the scraping tool out of the module shell 1 mm to collect and return tissue into the shell. Triggering of the actuator can be achieved in under 5 s where total actuation occurs in < 1 s. The module is capable of 2.5 N force output and collection of 0.4-2.8 mm^3 of intestinal tissue while only requiring a power output of less than 150-180 mW. Future work will include the development of sealing and preservation components of the device to ensure the proper protection of the sample for evaluation after exiting the body. The low power requirements of the module facilitate facile integration with a full ingestible device featuring sensors for localization and remote triggering. Miniaturization of the capsule prototype to an ingestible form factor of 9.9 mm x 26 mm is imperative for clinical translation. The roadmap toward achieving miniaturization must include: (1) exploring material selection for achieving more robust mechanical components to reduce the biopsy module footprint; (2) redesigning the PCB and utilizing smaller batteries to reduce the overall capsule diameter; (3) utilization of a more compact torque source reducing capsule length. Moreover, an evaluation of system reliability in a dynamic phantom or ex vivo environment is necessary for ensuring proper sample collection. Further development of this technology will enable autonomously operated capsule devices that could help reduce the burden of GI healthcare screening. Overall, this work will enable remote biopsy of tissue from an ingestible capsule, providing a minimally invasive method of GI disease monitoring.

Acknowledgment

The authors acknowledge support from the Clark Doctoral Fellows Program, TerrapinWorks, the University of Maryland NanoCenter, and its FabLab.

References

[1] Y. Wang et al., "Global burden of digestive diseases: A systematic analysis of the global burden of diseases study, 1990 to 2019," *Gastroenterology*, vol. 165, no. 3, pp. 773–783.e15, Sep. 2023, doi: 10.1053/j.gastro.2023.05.050.

[2] V. Jairath and B. G. Feagan, "Global burden of inflammatory bowel disease," *Lancet Gastroenterology Hepatology*, vol. 5, no. 1, pp. 2–3, Jan. 2020, doi: 10.1016/s2468-1253(19)30358-9.

[3] C. J. Black, D. A. Drossman, N. J. Talley, J. Ruddy, and A. C. Ford, "Functional gastrointestinal disorders: Advances in understanding and management," *Lancet*, vol. 396, no. 10263, pp. 1664–1674, Nov. 2020, doi: 10.1016/s0140-6736(20)32115-2.

[4] D. S. Levine, R. C. Haggitt, P. L. Blount, P. S. Rabinovitch, V. W. Rusch, and B. J. Reid, "An endoscopic biopsy protocol can differentiate high-grade dysplasia from early adenocarcinoma in Barrett's esophagus," *Gastroenterology*, vol. 105, no. 1, pp. 40–50, Jul. 1993.

[5] I. Aziz and M. Simrén, "The overlap between irritable bowel syndrome and organic gastrointestinal diseases," *Lancet Gastroenterology Hepatology*, vol. 6, no. 2, pp. 139–148, Feb. 2021, doi: 10.1016/s2468-1253(20)30212-0.

[6] N. D. Bortoli et al., "Gastroesophageal reflux disease, functional dyspepsia and irritable bowel syndrome: Common overlapping gastrointestinal disorders," *Ann. Gastroenterology*, vol. 31, no. 6, pp. 639–648, Nov. 2018, doi: 10.20524/aog.2018.0314.

[7] T. Matsui et al., "Clinical features and pattern of indeterminate colitis: Crohn's disease with ulcerative colitis-like clinical presentation," *J. Gastroenterology*, vol. 38, no. 7, pp. 647–655, Jul. 2003, doi: 10.1007/s00535-003-1117-8.

[8] C. Le Berre, A. N. Ananthakrishnan, S. Danese, S. Singh, and L. Peyrin-Biroulet, "Ulcerative colitis and Crohn's disease have similar burden and goals for treatment," *Clin. Gastroenterology Hepatology*, vol. 18, no. 1, pp. 14–23, Jan. 2020, doi: 10.1016/j.cgh.2019.07.005.

[9] P. Cortegoso Valdivia et al., "Clinical feasibility of panintestinal (or panenteric) capsule endoscopy: A systematic review," *Eur. J. Gastroenterology Hepatology*, vol. 33, no. 7, pp. 949–955, Jul. 2021, doi: 10.1097/meg.0000000000002200.

[10] B. M. Wiarda et al., "Patient burden and patient preference: Comparing magnetic resonance enteroclysis, capsule endoscopy and balloon-assisted enteroscopy," *J. Gastroenterology Hepatology*, vol. 28, no. 3, pp. 464–471, Mar. 2013, doi: 10.1111/j.1440-1746.2012.07223.x.

[11] H. Ojidu et al., "Patient tolerance and acceptance of different colonic imaging modalities: An observational cohort study," *Eur. J. Gastroenterology Hepatology*, vol. 30, no. 5, pp. 520–525, May 2018, doi: 10.1097/meg.0000000000001090.

[12] A. Lahat et al., "Magnetic resonance enterography or video capsule endoscopy—What do Crohn's disease patients prefer?," *Patient Preference Adherence*, vol. 2016, p. 1043, Jun. 2016, doi: 10.2147/ppa.s99690.

[13] W. H. Crosby, U. S. Army, and H. W. Kugler, "Intraluminal biopsy of the small intestine: The intestinal biopsy capsule," *Amer. J. Digestive Diseases*, vol. 2, no. 5, pp. 236–241, May 1957, doi: 10.1007/bf02231100.

[14] L. A. Beardslee et al., "Ingestible sensors and sensing systems for minimally invasive diagnosis and monitoring: The next frontier in minimally invasive screening," *ACS Sensors*, vol. 5, no. 4, pp. 891–910, Apr. 2020, doi: 10.1021/acssensors.9b02263.

[15] S. N. Adler and Y. C. Metzger, "PillCam COLON capsule endoscopy: Recent advances and new insights," *Therapeutic Adv. Gastroenterology*, vol. 4, no. 4, pp. 265–268, Jul. 2011, doi: 10.1177/1756283x11401645.

[16] D. Majumdar, R. Sidhu, A. J. Lobo, and M. E. McAlindon, "Pillcam colon capsule is an effective tool in management of patients with suspected or known inflammatory bowel disease: Preliminary results from a U.K. tertiary care centre," *Gut*, vol. 60, no. 1, p. A209, Apr. 2011, doi: 10.1136/gut.2011.239301.441.

[17] C. Spada et al., "Accuracy and safety of second-generation PillCam COLON capsule for colorectal polyp detection," *Therapeutic Adv. Gastroenterology*, vol. 5, no. 3, pp. 173–178, May 2012, doi: 10.1177/1756283x12438054.

[18] M. Koziolek et al., "Investigation of pH and temperature profiles in the GI tract of fasted human subjects using the Intellicap® system," *J. Pharmaceutical Sci.*, vol. 104, no. 9, pp. 2855–2863, Sep. 2015, doi: 10.1002/jps.24274.

[19] M. O. Tokhi and G. S. Virk, *Advances in Cooperative Robotics: Proceedings of the 19th International Conference on CLAWAR 2016*. Singapore: World Scientific, 2016, doi: 10.1142/10261.

[20] Z. Song, W. Zhang, W. Zhang, and D. Paolo, "A novel biopsy capsule robot based on high-speed cutting tissue," *Cyborg Bionic Syst.*, vol. 2022, pp. 2022–9783517, Jan. 2022, doi: 10.34133/2022/9783517.

[21] K. Kong, S. Yim, S. Choi, and D. Jeon, "A robotic biopsy device for capsule endoscopy," *J. Med. Devices*, vol. 6, no. 3, Sep. 2012, Art. no. 031004, doi: 10.1115/1.4007100.

[22] M. Hoang et al., "A robotic biopsy endoscope with magnetic 5-DOF locomotion and a retractable biopsy punch," *Micromachines*, vol. 11, no. 1, p. 98, Jan. 2020, doi: 10.3390/mi11010098.

Authorized licensed use limited to: University of Maryland College Park. Downloaded on July 02,2026 at 20:38:50 UTC from IEEE Xplore. Restrictions apply.

This article has been accepted for inclusion in a future issue of this journal. Content is final as presented, with the exception of pagination.

[23] P. Zhu, H. Peng, and J. Yang, "Analyses of the temperature field of a piezoelectric micro actuator in the endoscopic biopsy channel," *Appl. Sci.*, vol. 9, no. 21, p. 4499, Oct. 2019, doi: 10.3390/app9214499.

[24] S. Yim, E. Gultepe, D. H. Gracias, and M. Sitti, "Biopsy using a magnetic capsule endoscope carrying, releasing, and retrieving untethered microgrippers," *IEEE Trans. Biomed. Eng.*, vol. 61, no. 2, pp. 513–521, Feb. 2014, doi: 10.1109/TBME.2013.2283369.

[25] M. Rehan, I. Al-Bahadly, D. G. Thomas, and E. Avci, "Capsule robot for gut microbiota sampling using shape memory alloy spring," *Int. J. Med. Robot. Comput. Assist. Surgery*, vol. 16, no. 5, pp. 1–14, Oct. 2020, doi: 10.1002/rcs.2140.

[26] D. Ye et al., "Design and control of a magnetically-actuated capsule robot with biopsy function," *IEEE Trans. Biomed. Eng.*, vol. 69, no. 9, pp. 2905–2915, Sep. 2022, doi: 10.1109/TBME.2022.3157451.

[27] M. Finocchiaro et al., "Design of a magnetic actuation system for a microbiota-collection ingestible capsule," in *Proc. IEEE Int. Conf. Robot. Autom. (ICRA)*, May 2021, pp. 6905–6911, doi: 10.1109/ICRA48506.2021.9561142.

[28] F. Zhang, D. Ye, S. Song, and M. Q.-H. Meng, "Design of a novel biopsy capsule robot with anchoring function for intestinal tract," in *Proc. IEEE Int. Conf. Robot. Biomimetics (ROBIO)*, Dec. 2019, pp. 1471–1476, doi: 10.1109/ROBIO49542.2019.8961585.

[29] J. Gao, G. Yan, S. He, F. Xu, and Z. Wang, "Design, analysis, and testing of a motor-driven capsule robot based on a sliding clamper," *Robotica*, vol. 35, no. 3, pp. 521–536, Mar. 2017, doi: 10.1017/s0263574715000697.

[30] V. H. Le et al., "Electromagnetic field intensity triggered micro-biopsy device for active locomotive capsule endoscope," *Mechatronics*, vol. 36, pp. 112–118, Jun. 2016, doi: 10.1016/j.mechatronics.2016.05.001.

[31] T. Matsui, S. Murata, and T. Honda, "Fabrication of magnetically driven biopsy mechanism applicable to capsule-type medical device," *J. Robot. Mechatronics*, vol. 30, no. 2, pp. 292–299, Apr. 2018, doi: 10.20965/jrm.2018.p0292.

[32] M. Simi, G. Gerboni, A. Menciassi, and P. Valdastri, "Magnetic torsion spring mechanism for a wireless biopsy capsule," *J. Med. Devices*, vol. 7, no. 4, Dec. 2013, Art. no. 041009, doi: 10.1115/1.4025185.

[33] D. Son, H. Gilbert, and M. Sitti, "Magnetically actuated soft capsule endoscope for fine-needle biopsy," *Soft Robot.*, vol. 7, no. 1, pp. 10–21, Feb. 2020, doi: 10.1089/soro.2018.0171.

[34] D. Ye, F. Zhang, S. Yuan, S. Song, and M. Q.-H. Meng, "Magnetically driven wireless capsule robot with targeting biopsy function," in *Proc. IEEE Int. Conf. Robot. Biomimetics (ROBIO)*, Dec. 2019, pp. 1222–1227, doi: 10.1109/ROBIO49542.2019.8961521.

[35] K. Hajima, M. Yamashita, and T. Honda, "Performance evaluation of magnetically driven cytology brush applicable to capsule endoscopy," *Int. J. Appl. Electromagn. Mech.*, vol. 50, no. 1, pp. 167–176, Jan. 2016, doi: 10.3233/jae-150101.

[36] W. Zhang, P. Dario, W. Zhang, and Z. Song, "Positioning and posture adjustment for a rotational cutting biopsy capsule," in *Proc. Int. Conf. Adv. Robot. Mechatronics (ICARM)*, Guilin, China, Jul. 2022, pp. 82–86, doi: 10.1109/ICARM54641.2022.9959130.

[37] V. H. Le et al., "Shape memory alloy–based biopsy device for active locomotive intestinal capsule endoscope," *Proc. Inst. Mech. Eng., H, J. Eng. Med.*, vol. 229, no. 3, pp. 255–263, Mar. 2015, doi: 10.1177/0954411915576946.

[38] M. J. Gora et al., "Tethered capsule endomicroscopy enables less invasive imaging of gastrointestinal tract microstructure," *Nature Med.*, vol. 19, no. 2, pp. 238–240, Feb. 2013, doi: 10.1038/nm.3052.

[39] C. Quaglia, S. Tognarelli, E. Sinibaldi, N. Funaro, P. Dario, and A. Menciassi, "Wireless robotic capsule for releasing bioadhesive patches in the gastrointestinal tract," *J. Med. Devices*, vol. 8, no. 1, Mar. 2014, Art. no. 014503, doi: 10.1115/1.4025450.

[40] H. L. Kaan, P. T. Phan, A. M. H. Tiong, M. Miyasaka, S. J. Phee, and K. Y. Ho, "First-in-man feasibility study of a novel ingestible magnetically inflated balloon capsule for treatment of obesity," *Endoscopy Int. Open*, vol. 8, no. 5, pp. E607–E610, May 2020, doi: 10.1055/a-1127-2991.

[41] M. Simi, P. Valdastri, C. Quaglia, A. Menciassi, and P. Dario, "Design, fabrication, and testing of a capsule with hybrid locomotion for gastrointestinal tract exploration," *IEEE/ASME Trans. Mechatronics*, vol. 15, no. 2, pp. 170–180, Apr. 2010, doi: 10.1109/TMECH.2010.2041244.

[42] S. V. Hoffmann, B. T. Griffin, V. Jannin, and J. P. O'Shea, "Evaluating drug absorption from enteric capsules in pigs: Impact of capsule size on gastric emptying," *Eur. J. Pharmaceutical Sci.*, vol. 213, Oct. 2025, Art. no. 107237, doi: 10.1016/j.ejps.2025.107237.

[43] Z. Li et al., "Rotating multibarreled capsule robot for multiple biopsies and on-demand drug delivery," *IEEE/ASME Trans. Mechatronics*, vol. 30, no. 6, pp. 7089–7099, Dec. 2025, doi: 10.1109/TMECH.2025.3532617.

[44] L. Song et al., "Motion control of capsule robot based on adaptive magnetic levitation using electromagnetic coil," *IEEE Trans. Autom. Sci. Eng.*, vol. 20, no. 4, pp. 2720–2731, Oct. 2023, doi: 10.1109/TASE.2022.3201966.

[45] F. Wang, J. Yang, L. Song, and L. Feng, "Levitation control of capsule robot with 5-DOF based on arrayed Hall elements," in *Proc. Int. Conf. Manipulation, Autom. Robot. at Small Scales (MARSS)*, Toronto, ON, Canada, Jul. 2022, pp. 1–6, doi: 10.1109/MARSS55884.2022.9870460.

[46] K. M. Popek, T. Hermans, and J. J. Abbott, "First demonstration of simultaneous localization and propulsion of a magnetic capsule in a lumen using a single rotating magnet," in *Proc. IEEE Int. Conf. Robot. Autom. (ICRA)*, May 2017, pp. 1154–1160, doi: 10.1109/ICRA.2017.7989138.

[47] Y. Xu, K. Li, Z. Zhao, and M. Q.-H. Meng, "On reciprocally rotating magnetic actuation of a robotic capsule in unknown tubular environments," *IEEE Trans. Med. Robot. Bionics*, vol. 3, no. 4, pp. 919–927, Nov. 2021, doi: 10.1109/TMRB.2021.3123407.

[48] M. Rehan, I. Al-Bahadly, D. G. Thomas, and E. Avci, "Towards gut microbiota sampling using an untethered sampling device," *IEEE Access*, vol. 9, pp. 127175–127184, 2021, doi: 10.1109/ACCESS.2021.3111086.

[49] S. Park, K.-I. Koo, S. M. Bang, J. Y. Park, S. Y. Song, and D. D. Cho, "A novel microactuator for microbiopsy in capsular endoscopes," *J. Micromech. Microeng.*, vol. 18, no. 2, Feb. 2008, Art. no. 025032, doi: 10.1088/0960-1317/18/2/025032.

[50] S. Park et al., "A novel micro-biopsy actuator for capsular endoscope using LIGA process," in *Proc. Int. Solid-State Sensors, Actuators Microsystems Conf.*, Jun. 2007, pp. 209–212, doi: 10.1109/SENSOR.2007.4300107.

[51] M. A. Straker, J. Levy, and R. Ghodssi, "Low-power thermomechanical module for targeted ingestible device biopsy," in *Proc. Solid-State, Actuat., Microsystems Workshop Tech. Dig.*, Jun. 2024, pp. 459–460.

[52] J. A. Levy, M. A. Straker, J. M. Stine, L. A. Beardslee, V. Borbash, and R. Ghodssi, "Thermomechanical soft actuator for targeted delivery of anchoring drug deposits to the GI tract," *Adv. Mater. Technol.*, vol. 8, no. 2, Jan. 2023, Art. no. 2201365, doi: 10.1002/admt.202201365.

[53] L. Barducci et al., "Fundamentals of the gut for capsule engineers," *Prog. Biomed. Eng.*, vol. 2, no. 4, Sep. 2020, Art. no. 042002, doi: 10.1088/2516-1091/abab4c.

[54] P. A. van Riet et al., "Combined versus single use 20 G fine-needle biopsy and 25 G fine-needle aspiration for endoscopic ultrasound-guided tissue sampling of solid gastrointestinal lesions," *Endoscopy*, vol. 52, no. 1, pp. 37–44, Jan. 2020, doi: 10.1055/a-0966-8755.

[55] M. Sekine, T. Asano, and H. Mashima, "The diagnosis of small gastrointestinal subepithelial lesions by endoscopic ultrasound-guided fine needle aspiration and biopsy," *Diagnostics*, vol. 12, no. 4, p. 810, Mar. 2022, doi: 10.3390/diagnostics12040810.

[56] Y. M. Xie, S. Xu, C. S. Zhang, and C. C. Xue, "Examination of surface conditions and other physical properties of commonly used stainless steel acupuncture needles," *Acupuncture Med.*, vol. 32, no. 2, pp. 146–154, Apr. 2014, doi: 10.1136/acupmed-2013-010472.

[57] E. J. Poveda-Pagán, S. Hernández-Sánchez, L. Rhys-Jones-López, A. Palazón-Bru, and C. Lozano-Quijada, "Scanning electron microscopy examination of needle tips after different procedures of deep dry needling in humans," *Sci. Rep.*, vol. 8, no. 1, p. 17966, Dec. 2018, doi: 10.1038/s41598-018-36417-w.

[58] M. Giovannini, H. Ren, X. Wang, and K. Ehmann, "Tissue cutting with microserrated biopsy punches," *J. Micro Nano-Manuf.*, vol. 5, no. 4, Dec. 2017, Art. no. 041004, doi: 10.1115/1.4037726.

[59] P. Han, D. Che, K. Pallav, and K. Ehmann, "Models of the cutting edge geometry of medical needles with applications to needle design," *Int. J. Mech. Sci.*, vol. 65, no. 1, pp. 157–167, Dec. 2012, doi: 10.1016/j.ijmecsci.2012.09.014.

[60] C. T. McCarthy, M. Hussey, and M. D. Gilchrist, "On the sharpness of straight edge blades in cutting soft solids: Part I—Indentation experiments," *Eng. Fract. Mech.*, vol. 74, no. 14, pp. 2205–2224, Sep. 2007, doi: 10.1016/j.engfracmech.2006.10.015.

[61] T. Koch et al., "Approaching standardization: Mechanical material testing of macroscopic two-photon polymerized specimens," *Adv. Mater.*, vol. 36, no. 34, Aug. 2024, Art. no. 2308497, doi: 10.1002/adma.202308497.

Authorized licensed use limited to: University of Maryland College Park. Downloaded on July 02,2026 at 20:38:50 UTC from IEEE Xplore. Restrictions apply.

This article has been accepted for inclusion in a future issue of this journal. Content is final as presented, with the exception of pagination.

[62] S. Sarker et al., "3D-printed microinjection needle arrays via a hybrid DLP-direct laser writing strategy," *Adv. Mater. Technol.*, vol. 8, no. 5, Mar. 2023, Art. no. 2201641, doi: 10.1002/admt.202201641.
[63] A. Mishra and R. O. Cleveland, "Agarose as a tissue mimic for the porcine heart, kidney, and liver: Measurements and a springpot model," *Bioengineering*, vol. 11, no. 6, p. 589, Jun. 2024, doi: 10.3390/bioengineering11060589.
[64] M. Navarro-Lozoya, M. S. Kennedy, D. Dean, and J. I. Rodriguez-Devora, "Development of phantom material that resembles compression properties of human brain tissue for training models," *Materialia*, vol. 8, Dec. 2019, Art. no. 100438, doi: 10.1016/j.mtla.2019.100438.
[65] J. Bauer et al., "Increased stiffness of the tumor microenvironment in colon cancer stimulates cancer associated fibroblast-mediated prometastatic activin a signaling," *Sci. Rep.*, vol. 10, no. 1, p. 50, Jan. 2020, doi: 10.1038/s41598-019-55687-6.
[66] L. A. Johnson et al., "Matrix stiffness corresponding to strictured bowel induces a fibrogenic response in human colonic fibroblasts," *Inflammatory Bowel Diseases*, vol. 19, no. 5, pp. 891–903, Apr. 2013, doi: 10.1097/mib.0b013e3182813297.
[67] D. C. Stewart et al., "Quantitative assessment of intestinal stiffness and associations with fibrosis in human inflammatory bowel disease," *PLoS ONE*, vol. 13, no. 7, Jul. 2018, Art. no. e0200377, doi: 10.1371/journal.pone.0200377.
[68] L. G. Ponsaing, "Diagnostic procedures for submucosal tumors in the gastrointestinal tract," *World J. Gastroenterology*, vol. 13, no. 24, p. 3301, 2007, doi: 10.3748/wjg.v13.i24.3301.
[69] A. Ed-Daoui, M. Benelmostafa, and M. Dahmani, "Study of the viscoelastic properties of the agarose gel," *Mater. Today, Proc.*, vol. 13, pp. 746–751, Apr. 2019, doi: 10.1016/j.matpr.2019.04.036.
[70] V. Vullo, "Gears: General concepts, definitions and some basic quantities," in *Gears: Volume 1: Geometric and Kinematic Design*, vol. 10. Cham, Switzerland: Springer, 2020, pp. 1–38, doi: 10.1007/978-3-030-36502-81.
[71] J. M. D. Castillo, "The analytical expression of the efficiency of planetary gear trains," *Mechanism Mach. Theory*, vol. 37, no. 2, pp. 197–214, Feb. 2002, doi: 10.1016/s0094-114x(01)00077-5.
[72] J. A. Levy, M. A. Straker, J. M. Stine, L. A. Beardslee, and R. Ghodssi, "Magnetically triggered ingestible capsule for localized microneedle drug delivery," *Device*, vol. 2, no. 10, Oct. 2024, Art. no. 100438, doi: 10.1016/j.device.2024.100438.
[73] M. A. Moyano, R. París, and J. M. Martín-Martínez, "Viscoelastic and adhesion properties of hot-melts made with blends of ethylene-co-n-butyl acrylate (EBA) and ethylene-co-vinyl acetate (EVA) copolymers," *Int. J. Adhes. Adhesives*, vol. 88, pp. 34–42, Jan. 2019, doi: 10.1016/j.ijadhadh.2018.11.001.
[74] P. Fleckenstein, "Migrating electrical spike activity in the fasting human small intestine," *Amer. J. Digestive Diseases*, vol. 23, no. 9, pp. 769–775, Sep. 1978, doi: 10.1007/bf01079784.
[75] L. Liu, S. Towfighian, and A. Hila, "A review of locomotion systems for capsule endoscopy," *IEEE Rev. Biomed. Eng.*, vol. 8, pp. 138–151, 2015, doi: 10.1109/RBME.2015.2451031.
[76] D. Kulling, D. Bohning, C. Kay, D. Feldman, P. Cotton, and R. Hawes, "Histological correlates to pig gastrointestinal wall layers imaged in vitro with the magnetic resonance endoscope," *Gastroenterology*, vol. 112, no. 5, pp. 1568–1574, May 1997, doi: 10.1016/s0016-5085(97)70038-6.
[77] L. S. Wood, H. S. Hosseini, M. Diyaolu, A.-L. Thomas, J. S. Taylor, and J. C. Dunn, "Mechanical lengthening of porcine small intestine with decreased forces," *J. Pediatric Surgery*, vol. 56, no. 7, pp. 1192–1198, Jul. 2021, doi: 10.1016/j.jpedsurg.2021.03.036.
[78] M. Macari and E. J. Balthazar, "CT of bowel wall thickening: Significance and pitfalls of interpretation," *Amer. J. Roentgenology*, vol. 176, no. 5, pp. 1105–1116, May 2001, doi: 10.2214/ajr.176.5.1761105.
[79] H. S. Hosseini and J. C. Y. Dunn, "Biomechanical force prediction for lengthening of small intestine during distraction enterogenesis," *Bioengineering*, vol. 7, no. 4, p. 140, Nov. 2020, doi: 10.3390/bioengineering7040140.
[80] M. N. Marsh and J. A. Swift, "A study of the small intestinal mucosa using the scanning electron microscope," *Gut*, vol. 10, no. 11, pp. 940–949, Nov. 1969, doi: 10.1136/gut.10.11.940.
[81] D. U. Silverthorn, B. R. Johnson, W. C. Ober, C. E. Ober, and A. C. Silverthorn, *Human Physiology: An Integrated Approach*, 7th ed., San Francisco, CA, USA: Pearson, 2016.
[82] V. Villanacci et al., "Histopathology of IBD colitis. A practical approach from the pathologists of the Italian group for the study of the gastrointestinal tract (GIPAD)," *Pathologica*, vol. 113, no. 1, pp. 39–53, Feb. 2021, doi: 10.32074/1591-951x-235.
[83] H. J. Freeman, "Role of biopsy in diagnosis and treatment of adult celiac disease," *Gastroenterol. Hepatol. Bed Bench*, vol. 11, no. 3, pp. 191–196, 2016.
[84] C. Catassi and A. Fasano, "Celiac disease diagnosis: Simple rules are better than complicated algorithms," *Amer. J. Med.*, vol. 123, no. 8, pp. 691–693, Aug. 2010, doi: 10.1016/j.amjmed.2010.02.019.
[85] A. Hopper, S. Cross, and D. Sanders, "Patchy villous atrophy in adult patients with suspected gluten-sensitive enteropathy: Is a multiple duodenal biopsy strategy appropriate?," *Endoscopy*, vol. 40, no. 3, pp. 219–224, Mar. 2008, doi: 10.1055/s-2007-995361.
[86] D. H. Dewar and P. J. Ciclitira, "Clinical features and diagnosis of celiac disease," *Gastroenterology*, vol. 128, no. 4, pp. S19–S24, Apr. 2005, doi: 10.1053/j.gastro.2005.02.010.
[87] M. D. Hale, T. Gotoda, J. D. Hayden, and H. I. Grabsch, "Endoscopic biopsies from gastrointestinal carcinomas and their suitability for molecular analysis: A review of the literature and recommendations for clinical practice and research," *Histopathology*, vol. 67, no. 2, pp. 147–157, Aug. 2015, doi: 10.1111/his.12626.
[88] G. S. Hirst, S. Sarker, and B. S. Terry, "Differences in the mechanical properties of intestinal tissue based on preservation freezing duration and temperature," *J. Mech. Behav. Biomed. Mater.*, vol. 152, Apr. 2024, Art. no. 106440, doi: 10.1016/j.jmbbm.2024.106440.
[89] J. M. Stine et al., "Miniaturized capsule system toward real-time electrochemical detection of H_2S in the gastrointestinal tract," *Adv. Healthcare Mater.*, vol. 13, no. 5, Feb. 2024, Art. no. 2302897, doi: 10.1002/adhm.202302897.
[90] M. W. Lim, B. M. Holt, J. A. Levy, J. M. Stine, L. A. Beardslee, and R. Ghodssi, "Ingestible bioimpedance sensing device for localized feedback-driven drug delivery," in *Proc. Solid-State, Sensors, Actuators, Microsystems Workshop*, Jun. 2024, pp. 114–115.
[91] K.-C. Kong, J. Cha, D. Jeon, and D.-I. D. Cho, "A rotational micro biopsy device for the capsule endoscope," in *Proc. IEEE/RSJ Int. Conf. Intell. Robots Syst.*, May 2005, pp. 1839–1843, doi: 10.1109/IROS.2005.1545441.
[92] B. S. Terry, J. A. Schoen, and M. E. Rentschler, "Characterization and experimental results of a novel sensor for measuring the contact force from myenteric contractions," *IEEE Trans. Biomed. Eng.*, vol. 59, no. 7, pp. 1971–1977, Jul. 2012, doi: 10.1109/TBME.2012.2195179.
[93] B. S. Terry, J. A. Schoen, and M. E. Rentschler, "Measurements of the contact force from myenteric contractions on a solid bolus," *J. Robotic Surgery*, vol. 7, no. 1, pp. 53–57, Mar. 2013, doi: 10.1007/s11701-012-0346-3.
[94] S. Nejati et al., "Electronic-free traceable smart capsule for gastrointestinal microbiome sampling," *Adv. Mater. Technol.*, vol. 9, no. 6, Mar. 2024, Art. no. 2300810, doi: 10.1002/admt.202300810.
[95] S. Nejati et al., "Small intestinal sampling capsule for inflammatory bowel disease type detection and management," *Lab Chip*, vol. 22, no. 1, pp. 57–70, 2022, doi: 10.1039/d1lc00451d.
[96] M. A. Straker, J. A. Levy, J. M. Stine, V. Borbash, L. A. Beardslee, and R. Ghodssi, "Freestanding region-responsive bilayer for functional packaging of ingestible devices," *Microsystems Nanoengineering*, vol. 9, no. 1, p. 61, May 2023, doi: 10.1038/s41378-023-00536-w.
[97] B. J. Wood, J. R. Ramkaransingh, T. Fojo, M. M. Walther, and S. K. Libutti, "Percutaneous tumor ablation with radiofrequency," *Cancer*, vol. 94, no. 2, pp. 443–451, Jan. 2002, doi: 10.1002/cncr.10234.
[98] L. Jäger, E. Morales-Orcajo, A. Gager, A. Bader, A. Dillinger, and A. Blutke, "Preclinical assessment of tissue effects by gastrointestinal endoscope tip temperature," *Current Therapeutic Res.*, vol. 98, Feb. 2023, Art. no. 100693, doi: 10.1016/j.curtheres.2023.100693.

Michael A. Straker received the B.S. degree in bioengineering from Temple University, Philadelphia, PA, USA, in 2016, the M.S. degree in integrated sciences-physics from Morgan State University, Baltimore, MD, USA, in 2020, and the Ph.D. degree in bioengineering from the University of Maryland, College Park, MD, USA, in 2025. He is currently a Post-Doctoral Associate with the National Institute of Standards and Technology (NIST). The work presented was completed as part of his doctoral research focused on the development of ingestible technologies for localized tissue biopsy while affiliated with the University of Maryland, College Park. His research interests include novel biosensors, therapeutic strategies, and medical devices that improve disease detection, monitoring, and treatment.

Authorized licensed use limited to: University of Maryland College Park. Downloaded on July 02,2026 at 20:38:50 UTC from IEEE Xplore. Restrictions apply.

This article has been accepted for inclusion in a future issue of this journal. Content is final as presented, with the exception of pagination.

Joshua A. Levy received the B.S. degree in physics and the B.A. degree in chemistry from Binghamton University, Binghamton, NY, USA, in 2020, and the Ph.D. degree in materials science and engineering from the University of Maryland, College Park, MD, USA, in 2025. His doctoral research focused on the development of ingestible electronic devices for sensing and drug delivery applications, with an emphasis on micro-actuator development, additive manufacturing, and device integration. He contributed to the presented work while he was affiliated with the University of Maryland, College Park. He is currently a National Research Council (NRC) Post-Doctoral Researcher with U.S. Naval Research Laboratory (NRL), Washington, DC, USA, where he develops electrochemical sensing platforms, nanomaterial-enabled biosensors, electro-optical devices, and integrated electronic systems.

Anika Prasanna is currently pursuing the B.S. degree in bioengineering with the University of Maryland, College Park, MD, USA. She is researching hybrid energy harvesting methods for ingestible capsule devices. She will serve as a Summer Intern with the National Institute of Biomedical Imaging and Bioengineering (NIBIB), National Institutes of Health (NIH). Her research interests include bioelectronic devices, microsystems for physiological sensing, and biomedical device design. She has also contributed to projects involving intestinal physical models. Her long-term goal is to develop innovative biomedical technologies that improve accessibility in healthcare and engineering.

Patrick A. Sweeney received the B.S. degree in electrical engineering from the University of Maryland, College Park, in 2026. As an undergraduate researcher in the MEMS Sensors and Actuators Lab, he worked on the characterization and optimization of ingestible biopsy devices. His research interests include microelectronics, biosensing, and robotics.

Justin M. Stine (Member, IEEE) received the B.A. degree in physics and mathematics from the St. Mary's College of Maryland, St. Mary's City, MD, USA, in 2014, and the M.S. and Ph.D. degrees in electrical engineering from the University of Maryland, College Park, MD, USA, in 2019 and 2023, respectively. In 2023, he joined Maryland Autonomous Technologies Research Innovation and eXploration (MATRIX) Laboratory, University of Maryland, as an Assistant Research Scientist. He is an inventor on multiple patent applications related to ingestible sensing technologies, including wireless capsule systems for real-time bioprocess and bioimpedance monitoring. His work has also been featured on the cover of the journal *Advanced Healthcare Materials*. His research interests include ingestible bioelectronics, microsystems for physiological monitoring, autonomous sensing systems, and environmental monitoring technologies.

Luke A. Beardslee (Senior Member, IEEE) was born in Boston, MA, USA. He received the B.S. and M.Eng. degrees in electrical engineering from Cornell University, Ithaca, NY, USA, in 2007, the Ph.D. degree in electrical engineering from Georgia Institute of Technology, Atlanta, GA, USA, in 2011, and the M.D. degree from Albany Medical College, Albany, NY, USA, in 2015. He completed a general surgery internship with the Walter Reed National Military Medical Center, Bethesda, MD, USA, in 2016. He is an Electrical Engineer and a General Surgeon. From 2016 to 2020, he was an active duty Navy Undersea Medical Officer assigned to the Naval Submarine Medical Research Laboratory, Groton, CT, USA, where he worked on several projects including development of an ingestible blast sensing capsule and a wearable chemical sensing systems. From 2020 to 2025, he was a General Surgery Resident with the Emory University School of Medicine, Atlanta, GA, USA. During that time, he continued his research endeavors in the area of ingestible, implantable and wearable sensor, and actuator systems. He is currently a Surgical Critical Care Fellow with Penn State Hershey Medical Center, Hershey, PA, USA, and also a Research Affiliate with the Institute for Systems Research, University of Maryland, College Park. He is an author on multiple publication and an inventor on several patents related to embedded sensing technology, including ingestible capsule systems, gas sensing systems, and bioprocess monitoring. His research interests include micro/nanofabrication techniques, transducer development, and ingestible, implantable, and wearable sensors and sensing and actuation systems.

Reza Ghodssi (Fellow, IEEE) received the B.S., M.S., and Ph.D. degrees in electrical engineering from the University of Wisconsin–Madison, Madison, WI, USA, in 1990, 1992, and 1996, respectively. From 1996 to 1999, he was a Post-Doctoral Fellow and a Research Scientist working on microelectromechanical systems (MEMS) devices with Massachusetts Institute of Technology (MIT), Cambridge, MA, USA. Since 2000, he has been with the Department of Electrical and Computer Engineering (ECE), University of Maryland, College Park (UMD), MD, USA, where he is currently a Distinguished University Professor, the Herbert Rabin Distinguished Chair in Engineering, and a Distinguished Scholar Teacher. He is the Director of the MEMS Sensors and Actuators Laboratory (MSAL), jointly affiliated with the Department of Electrical and Computer Engineering and the Institute for Systems Research (ISR). He is the Inaugural Executive Director of research and innovation with the MATRIX Laboratory, UMD. He is the author or co-author of more than 181 journal publications and 381 refereed conference papers and the co-editor of the *MEMS Materials and Processes Handbook* (2011). He is an inventor on ten issued U.S. patents, 12 published U.S. patents, and five pending patent applications. His research interests include the design and development of micro-, nano-, and bio-devices and systems for chemical and biological sensors and actuators; and small-scale energy conversion and harvesting for healthcare applications. He is a fellow of AVS and ASME. Among his awards and recognitions, he received the 2024 American Vacuum Society (AVS) Gaede-Langmuir Award. He served as the President for the Transducer Research Foundation (TRF) from 2022 to 2026. He has served as the Chair and the Technical Program Chair for several national and international MEMS conferences, including 2022 and 2020 Hilton Head Workshops, respectively. He was the Lead Organizer and the Chair of the Inaugural Denice Denton Emerging Leaders Workshop 2016, which focused on helping mid-career faculty develop leadership skills, strategic networks, and professional advancement opportunities. He served as an Associate Editor for *Biomedical Microdevices* (BMMD) from 2008 to 2021 and *Journal of Microelectromechanical Systems* (JMEMS) from 2008 to 2020.

Authorized licensed use limited to: University of Maryland College Park. Downloaded on July 02,2026 at 20:38:50 UTC from IEEE Xplore. Restrictions apply.